CRYSTAL GROWTH OF PbO_2 AND ITS RELATION TO THE CAPACITY LOSS OF POSITIVE PLATES IN SEALED LEAD/ACID BATTERIES

J. YAMASHITA, H. YUFU and Y. MATSUMARU

Yuasa Battery Co., Ltd., 6-6 Josai-cho, Takatsuki, Osaka 569 (Japan)

Introduction

The demand for maintenance-free lead/acid batteries continues to grow following the establishment of practical 'sealed' technology based on the gas-recombination principle [1, 2]. In order to perfect this maintenance-free technology, it is necessary to gain a more complete understanding of the microstructure of the positive plate and its accompanying electrochemical behaviour [3]. Two models have been advanced for the microstructure of the positive-plate active material, namely, the 'α-PbO_2 network structure' [4, 5] and the 'coralloid structure' [6, 7]. Both models assert that the presence of antimony is essential for the particular structure to become well developed. Simon and Caulder [6, 7] proposed that 'amorphous PbO_2' and 'inactive PbO_2' are factors that control the electrochemical activity of PbO_2. According to Caulder: "The electrochemical activity of PbO_2 is controlled by the amount of hydrogen species which has made its way into the crystal latttice." During charge/discharge cycling, hydrogen atoms are lost from the crystal structure of PbO_2 and its electrochemical activity decreases. This is known as the 'hydrogen-loss' model, and Caulder further argues that: "The deviation from the stoichiometric ratio of PbO_2 (Pb:O = 1:2) is determined by the amount of H which makes its way into the PbO_2 crystal lattice." In this respect, the hydrogen-loss model may be regarded as basically the same as the $PbO_{2-\delta}(xH_2O)$ model formulated by Pohl and Rickert [8]. Pavlov *et al.* [9] have proposed a proton–electron mechanism for the $PbO_2/PbSO_4$ electrode reaction, and have reported that the hydrated layer of the PbO_2 crystal surface controls the electrochemical activity of host material. On the other hand, Hill *et al.* [10 - 12] have found that the amount of H making its way into the crystal lattice bears no direct relationship to the loss in PbO_2 capacity.

Experimental

Method for making test cell

Positive-plate paste was prepared by mixing 1 kg of Shimazu-mill leady oxide (72% PbO, 28% Pb) with 200 ml of 1.180 sp. gr. H_2SO_4. The paste was

0378-7753/90/$3.50

cured for 24 h at 35 °C and a relative humidity > 90%. Plate formation was carried out at 40 °C in 1.100 sp. gr. H_2SO_4 and at 13.8 A kg^{-1} of paste. Negative-plate paste was prepared in a similar fashion. The plates were 58 mm in height and 38 mm in width. Flooded cells were constructed by combining one positive plate and two negative plates with conventional glass-mat separators under conditions of no stacking pressure, and immersing the assembly in 100 ml of 1.300 sp. gr. H_2SO_4. A Pb–4.0wt.%Sb alloy was used to fabricate the positive grids for the control cells; grids in the remaining cells were made from Pb–0.08wt.%Ca–0.5wt.%Sn alloy. All the negative grids consisted of Pb–0.08wt.%Ca–0.5wt.%Sn alloy. Sealed cells were made by combining two positive plates and three negative plates with microfine glass-fibre mat separators under approximately 20 kg dm^{-2} stacking pressure, and immersing them in 40 ml of 1.300 sp. gr. H_2SO_4. The positive and negative grids were all made from Pb–0.08wt.%Ca–0.5wt.%Sn alloy.

Charge/discharge cycle testing

Testing of flooded and sealed lead/acid cells involved repeated charging and discharging at 40 °C to a discharge depth of 50%. After a given number of cycles, the positive plates were removed from the cell, washed with water, and dried at 55 °C. The morphology of the positive-plate active material was then examined by scanning electron microscopy using JEOL Model JSM-U3 and Model T-200 instruments. The specific surface area was measured with a Quantasorb specific surface-area analyzer (Quantachrome Corp.). The sample of active material was also separated from the grid and ground in an agate mortar to give particles of less than 10 μm in size. This powder was then subjected to X-ray diffraction (XRD) analysis using a Geigerflex Rad-IIA diffractometer (Rigaku Denki, Ltd.). The small amounts of PbO and $PbSO_4$ in the ground material were dissolved and removed in a solution of acetic acid and saturated ammonium sulphate at 50 °C. After this, the thermal decomposition characteristics of the PbO_2 were investigated with a Thermoflex 8085A instrument (Rigaku Denki, Ltd.). The distribution of $PbSO_4$ in the corrosion film surrounding the positive grid was investigated using a JSM-U3 and the EPMA method, as well as by optical examination with a metallurgical microscope (Olympus PMG-II).

Results and discussion

Deterioration mechanism of flooded lead/acid batteries

Microstructure of positive active material and PbO_2 morphology

The principal constituents of the positive-plate paste after curing were found to be tribasic lead sulphate ($3PbO{\cdot}PbSO_4{\cdot}H_2O$ = 3BS) and monobasic lead sulphate ($PbO{\cdot}PbSO_4$ = 1BS); no free lead sulphate was detected. The 3BS was present in the form of large crystals of length approximately 1.4 - 3.0 μm (Fig. 1(a)). The morphology of PbO_2 in a formed positive plate is

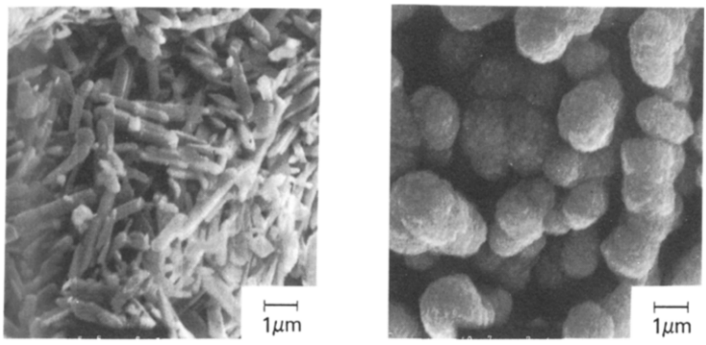

Fig. 1. Microstructure of (a) positive cured plate; (b) formed positive plate.

shown in Fig. 1(b). The average crystal size of β-PbO_2, as calculated from XRD data, was about 0.028 μm. The particle size calculated from the specific surface area of the material was about the same as that observed with a scanning electron microscope. Flooded cells using Pb–Ca–Sn and Pb–4.0wt.%Sb positive plates failed on the 14th and 69th cycles, respectively. The decline in capacity of the antimonial cells was due to the softening and shedding of the positive active material. Figure 2(a) and (b) shows the PbO_2 morphology in the failed plates in the two types of cell. Examination by scanning electron microscopy revealed that at the smallest size, PbO_2 had grown into prism-like crystals with lengths of about 0.3 and 0.8 μm in Pb–Ca–Sn and Pb–4.0wt.%Sb plates, respectively. By contrast, the corresponding average crystal sizes of β-PbO_2, calculated from XRD data, were $\sim$0.035 and $\sim$0.04 μm.

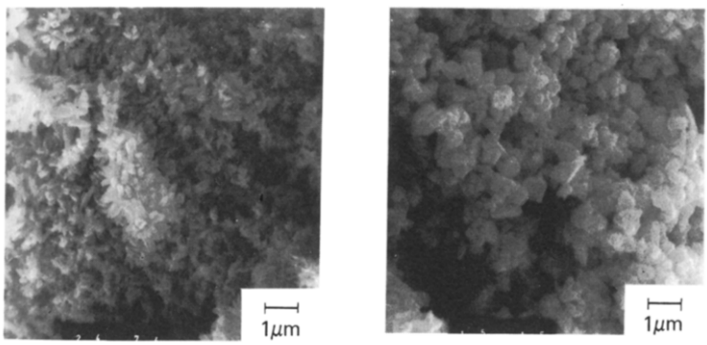

Fig. 2. Morphology of positive active material in failed flooded battery. (a) Pb–Ca–Sn positive plate before 15th discharge; (b) Pb–4.0wt.%Sb positive plate before 70th discharge.

Electrochemical behaviour of the grid corrosion film in Pb–Ca–Sn positive plates

Repeated charge/discharge cycling causes oxidation of the positive grid and the formation of a corrosion film. The positive active material is connected (or combined) with the grid metal by way of the corrosion film. The corrosion film on Pb–Ca–Sn alloy is less porous and has a finer microstructure than the film on a Pb–4.0wt.%Sb alloy, but because the film is not electrochemically inert, the charge/discharge reaction of the positive active material causes oxidation–reduction reactions within the corrosion zone. Figure 3 shows the $PbSO_4$ distribution, in a cross-sectional direction, in positive plates taken from flooded Pb–Ca–Sn batteries immediately before failure. After completion of the 14th discharge, the S Kα lines were 2 - 3 times stronger in the corrosion film than in the active material (Fig. 3(a)). This is considered to be the result of preferential $PbSO_4$ formation in the corrosion

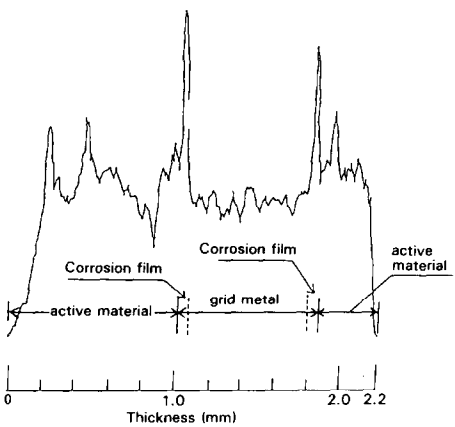

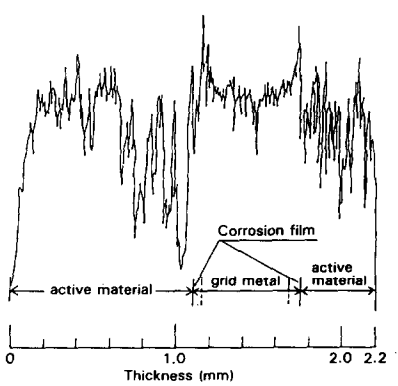

Fig. 3. $PbSO_4$ (S Kα radiation) distribution throughout cross section of positive active material and grid in flooded Pb–Ca–Sn battery. (a) At fully-discharged state in 14th cycle; (b) at fully-charged state in 15th cycle.

film during the process of discharging, so that when the active material discharges from PbO_2 to $PbSO_4$ the current is prevented from entering the grid metal of the collector. With further charging, the $PbSO_4$ layer formed on the corrosion film disappears and is almost completely restored to its former PbO_2 (Fig. 3(b)). Thus, in addition to the drastic softening and shedding of positive active material, the nature of the corrosion film with regard to its behaviour as a $PbSO_4$ barrier layer must be considered as a cause for the premature capacity loss of flooded Pb–Ca–Sn batteries when subjected to deep-discharge cycling service.

Deterioration mechanism of sealed lead/acid batteries

Microstructure of failed positive plates

Sealed lead/acid batteries use less electrolyte than flooded batteries, and the positive active material does not shed, even if it softens. This is because the batteries employ a smaller amount of electrolyte and have microfine glass-fibre mat separators. Figure 4(a) shows the morphology of positive active material from a sealed battery that failed after 710 cycles. It is considered that the PbO_2 has a morphology very much like that of the coralloid structure proposed by Caulder *et al.* [13]. According to Caulder, antimony is needed for the coralloid structure to become well developed. If it is assumed that such a structure results because antimony suppresses the softening and shedding of positive active material, then it is not unreasonable to conclude that a structure similar to a coralloid structure would also develop in the positive plates of sealed batteries. Figure 4(b) gives a magnified view of PbO_2 crystals with a coralloid structure. X-ray diffraction analysis showed that the positive active material consists of almost 100% β-PbO_2, with virtually no α-PbO_2 nor $PbSO_4$ being present. The average β-PbO_2 crystal particle size (calculated from the XRD peak) was

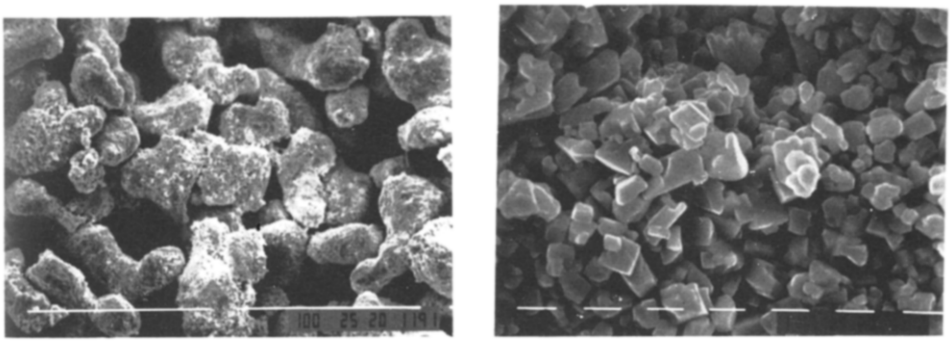

(a) (b)

Fig. 4. Microstructure of positive active material in flooded sealed battery before 710th discharge. (a) Microstructure similar to a 'coralloid structure'; (b) morphology of PbO_2 crystals which constitute a coralloid-like structure (a). (White lines correspond to: (a) 100 μm. (b) 1 μm.)

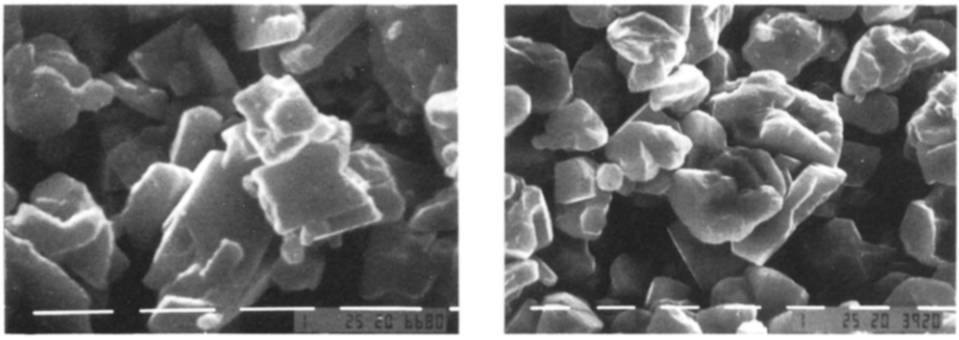

(a) (b)

Fig. 5. Large crystals of β-PbO_2 in positive active material in failed sealed battery. (a) β-PbO_2 crystals in positive plate before 1050th discharge; (b) β-PbO_2 with a twin crystal morphology. (White lines correspond to 1 μm.)

about 0.16 μm. With a scanning electron microscope, however, it was observed that crystals were, in fact, much larger and exceeded 2 μm in size; included within these crystals were some with a twin crystal morphology. Within present experimental limits, it has not been possible to observe PbO_2 crystals with a similar morphology in the positive plates of flooded cells (Figs. 4 and 5).

Thermal decomposition characteristics of PbO_2 in failed positive plates

The principal constituent of positive active material, β-PbO_2, forms crystals during repeated charge/discharge cycling. At failure, the particle size of β-PbO_2 is about 1.25 - 1.40 times, and about 5.7 times, the initial size in flooded cells and in sealed cells, respectively. On the other hand, the crystal growth rate, as observed with a scanning electron microscope, is considerably faster than that measured by XRD analysis, with the PbO_2 crystals in failed sealed cells having grown to 10 - 20 times the initial size. According to Caulder and Simon [14], Pavlov *et al.* [9], and Hill and Madsen [15], such PbO_2 crystal growth changes both the physical and the chemical properties of the material. Figure 6 shows the thermal decomposition patterns of PbO_2 in positive plates taken from failed flooded cells and sealed cells. As pointed out by Caulder and Simon [14], failed PbO_2 decomposes thermally into tet-PbO through almost the same process as chemically produced PbO_2, *i.e.*,

$$\beta\text{-}PbO_2 \xrightarrow{338\ ^\circ C} \alpha\text{-}PbO_x \xrightarrow{462\ ^\circ C} Pb_3O_4 \xrightarrow{590\ ^\circ C} \text{tet PbO}$$

Since the number of cycles required before failure differs appreciably between flooded cells and sealed cells, there is a considerable difference in the crystal particle sizes of the β-PbO_2. In spite of this, the PbO_2 thermal decomposition curves are almost the same. This suggests that the decomposition curve is little influenced by the increase in crystal particle size *per se* but more by changes in the PbO_2 crystal surface state, and the internal crystal

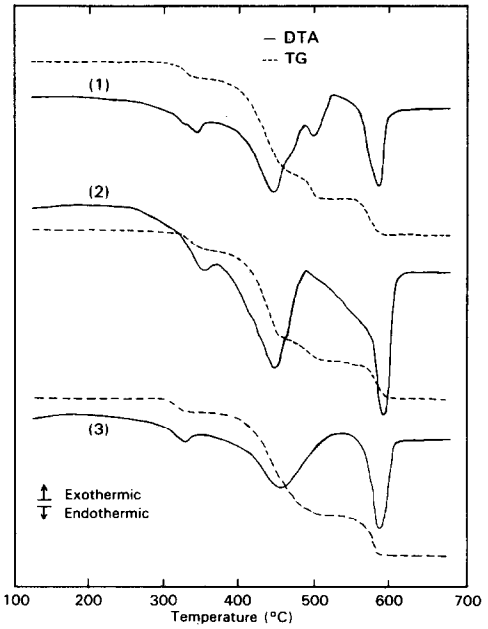

Fig. 6. DTA and TG curves of PbO_2 in failed positive active material at fully-charged state. (Reference sample: α-Al_2O_3, heating rate: 5 °C min^{-1}, atmosphere: air.) (1) PbO_2 in flooded Pb–Ca–Sn battery before 16th discharge. (2) PbO_2 in flooded Pb–4.0%Sb battery before 70th discharge. (3) PbO_2 in sealed battery before 558th discharge.

construction occurring in conjunction with crystal growth. There is still no adequate explanation, however, of why, when repeating a fixed number of charge/discharge cycles, the PbO_2 thermal decomposition curve shows a tendency to converge to almost the same pattern as failed PbO_2.

Relationship between PbO_2 crystal growth and diminishing capacity

Pavlov and Bashtavelova [16] have proposed that the mechanism of positive-plate deterioration in flooded cells consists of PbO_2 agglomerate structures changing into crystalline structures, and that this change causes the softening and shedding of positive active material. In sealed cells, however, the positive and negative plates are structured in such a way that they are subjected to about 20 kg dm^{-2} pressure in a cross-sectional direction so that the active material will not shed, even if it softens or swells. Thus, electrical contact is maintained physically between the PbO_2 particles of the positive active material, and PbO_2 crystal growth can continue for a longer period than in flooded batteries. Also, because the separators are pressed against the plates and because their pores are extremely small, oxygen gas evolving in the latter stage of charging moves primarily in a cross-sectional direction. Since, in sealed cells, the resistance toward the passage of oxygen gas through the interior of the positive active material is greater than that in flooded cells, the gas pressure is high. This situation is advantageous to the

formation of macropores in the interior of the positive active material and results in a well-developed coralloid structure. The mechanism by which the PbO_2 crystals themselves become large may be equated with the sintering process for ceramic materials, in which innumerable crystals of small particle size combine and grow into large crystals. The solubility of $PbSO_4$ in sulphuric acid is extremely low, being at best between 2×10^{-5} and 4×10^{-6} mol l^{-1}, so the rate at which the crystal boundary is lost is almost certainly very slow. If the mechanism by which the crystal boundary is lost proceeds by way of a dissolution–precipitation reaction through the medium of the solution, instead of a solid-state reaction, then H_2O will be taken into the crystal interior. On the other hand, though the enlargement of PbO_2 crystals is a matter of course, this reduces the specific surface area. As this reduces the free energy on the surfaces of PbO_2 crystals, it effects a corresponding reduction in the dissolution rate of Pb^{4+} ions. Conversely, the surfaces of the enlarged PbO_2 crystals are much smoother, and the degree of crystallization much greater, than in the early stage of the charge/discharge cycle. It is concluded, therefore, that these constitute major causes for the lowering of the electrochemical activity of PbO_2, ultimately leading to a decrease in positive-plate capacity.

Conclusions

The following conclusions can be drawn from the research results presented here:

(i) the decrease of positive-plate capacity in sealed lead/acid batteries, in which there is no shedding of positive active material, is due to advancing deactivation of the PbO_2 crystals themselves;

(ii) the decrease in the degree of PbO_2 electrochemical activity is closely related to changes in the surface state of the PbO_2 crystals, which are caused by crystal enlargement during charge/discharge cycling.

References

1 S. Sasabe, K. Yamasaki and Y. Kasai, *J. Power Sources, 19* (1987) 215.
2 S. Sasabe, M. Sasaki, K. Kishimoto, Y. Kasai and K. Fuchida, *ILZRO Battery Seminar, Osaka, Japan, June 3, 1988.*
3 J. Yamashita, Y. Matsumaru and A. Kita, *Yuasa Jiho, 58* (1985) 7.
4 J. Burbank, *Batteries, 1* (1962) 43.
5 A. C. Simon, *Batteries, 2* (1964) 63.
6 A. C. Simon and S. M. Caulder, in D. H. Collins (ed.), *Power Sources 5*, Academic Press, London, 1975, p. 109.
7 A. C. Simon, S. M. Caulder and T. Stemmle, *J. Electrochem. Soc., 122* (1975) 461.
8 J. P. Pohl and H. Rickert, in D. H. Collins (ed.), *Power Sources 5*, Academic Press, London, 1975, p. 15.
9 D. Pavlov, E. Bashtavelova, V. Manev and A. Nasalevska, *J. Power Sources, 19* (1987) 15.

10 R. J. Hill, A. M. Jessel and I. C. Madsen, in K. R. Bullock and D. Pavlov (eds.), *Symposium on Advances in Lead–Acid Batteries, New Orleans, 8 - 11 October, 1984*, The Electrochemical Society, Pennington, NJ, *Proc. Vol. 81-14*, 1985, pp. 59 - 77.
11 R. J. Hill and A. M. Jessel, *J. Electrochem. Soc., 134* (1987) 1326.
12 R. J. Hill, *J. Power Sources, 25* (1989) 313.
13 A. C. Simon, S. M. Caulder, C. P. Wales and R. J. Jones, *NRL Mem. Rep. 4751*, Feb. 26, 1982, pp. 74 - 84.
14 S. M. Caulder and A. C. Simon, *J. Electrochem. Soc., 121* (1974) 1546.
15 R. J. Hill and I. C. Madsen, *J. Electrochem. Soc., 131* (1984) 1486.
16 D. Pavlov and E. Bashtavelova, *J. Electrochem. Soc., 133* (1986) 241.